XTE J1118+480: A Metal-Rich Black Hole Binary in the Galactic Halo.

Jonay I. González Hernández[1,2,3], Rafael Rebolo[1,4], Garik Israelian[1], Emilios T. Harlaftis[5,6], Alexei V. Filippenko[7] and Ryan Chornock[7]

ABSTRACT

We present medium-resolution optical spectra of the secondary star in the high Galactic latitude black hole X-ray binary XTE J1118+480 and determine the abundance of Mg, Al, Ca, Fe, and Ni in its atmosphere. For all the elements investigated we find supersolar abundances; thus, we reject the hypothesis that the black hole came from the direct collapse of an ancient massive halo star. The compact primary most likely formed in a supernova event of a massive star whose nucleosynthetic products polluted the secondary star. The observed element abundances and their ratios can be explained using a variety of supernova models with a wide range of metallicities. While an explosive origin in the Galactic halo or thick disk cannot be discarded, a metal-rich progenitor is clearly favored by the observed abundance pattern. This suggests that the black hole was produced in the Galactic thin disk with a violent natal kick, propelling the X-ray binary to its current location and orbit.

Subject headings: black hole physics — stars: abundances — stars: evolution — stars: individual (XTE J1118+480) — supernovae: general — X-rays: binaries

1. Introduction

The low-mass X-ray binary XTE J1118+480 was discovered with the all-sky monitor aboard the Rossi X-ray Timing Explorer on UT 2000 March 29 (Remillard et al. 2000). Throughout its outburst the source remained in the low/hard state, one of the characteristic spectral states of an accreting black hole binary (McClintock et al. 2003). The system consists of a black hole with a mass estimated in the range 6−8 $M_\odot$ and a late-type secondary star of 0.1−0.5 $M_\odot$ (Wagner et al. 2001).

The extraordinarily high Galactic latitude ($b \approx 62.3°$), together with its distance of 1.85 ± 0.36 kpc (Wagner et al. 2001), places the system at a height of ∼1.6 kpc above the Galactic plane. In addition, an accurate measurement of its proper motion coupled with its distance provides space-velocity components U, V which seem consistent with those of some old halo globular clusters (Mirabel et al. 2001). If the system formed in the Galactic halo, the black hole could be either the remnant of a supernova in the very early Galaxy or the result of a direct collapse of an ancient massive star. However, the galactocentric orbit crossed the Galactic plane many times in the past, and an alternative possibility is that the system formed in the Galactic disk and was launched into its present orbit as a consequence of the "kick" acquired in the supernova explosion of a massive star (Gualandris et al. 2005). The metallicity of the secondary star may provide a key to distinguish among these two possible birth places, giving important clues to the formation of the black hole and the properties of

[1]Instituto de Astrofísica de Canarias, E-38205 La Laguna, Tenerife, Spain: jonay@iac.es, rrl@iac.es, gil@iac.es

[2]CIFIST Marie Curie Excellence Team

[3]Observatoire de Paris-Meudon, GEPI, 5 place Jules Janssen, 92195 Meudon Cedex, France

[4]Consejo Superior de Investigaciones Científicas, Spain

[5]Institute of Space Applications and Remote Sensing, National Observatory of Athens, PO Box 20048, Athens 118 10, Greece

[6]In memoriam

[7]Department of Astronomy, University of California, Berkeley, CA 94720-3411: alex@astro.berkeley.edu, chornock@astro.berkeley.edu

the supernova explosion, such as symmetry, released energy, and characteristics of the ejected matter (Israelian et al. 1999; Podsiadlowski et al. 2002).

2. Observations

We obtained 74 medium-resolution spectra ($\lambda/\delta\lambda \approx 6,000$) of the secondary star in XTE J1118+480, in quiescence, on UT 14 February 2004, using the 10-m Keck II telescope, equipped with the Echellette Spectrograph and Imager (ESI; Sheinis et al. 2002). The exposure time was fixed at 300 s to minimize the effects of orbital smearing which, for the orbital parameters of XTE J1118+480, is in the range 0.6–26.6 $\mathrm{km\,s^{-1}}$, smaller than the instrumental resolution of ~ 50 $\mathrm{km\,s^{-1}}$. Each individual spectrum was corrected for the radial velocity of the star, and the spectra were combined in order to improve the signal-to-noise ratio. After binning in wavelength in steps of 0.3 Å, the final spectrum had an average signal-to-noise ratio of 80 in the continuum. The data cover the spectral range 4000–9000 Å and clearly show the characteristic emission lines of accreting low-mass X-ray binaries (Balmer series and Ca II near-infrared triplet, He I 5876 Å, He I 6678 Å), superimposed on the typical photospheric spectrum of a late-type star.

3. Chemical Analysis

A comparison of the observed spectrum with the spectra of ten template stars (K0V–M2V) obtained with the same instrument allows us to classify the secondary as a mid to late K-type star. In Figure 1 we display two spectral regions containing some relevant lines for our analysis as well as a spectrum of a template star of similar spectral type for comparison with available detailed chemical analysis (Allende Prieto et al. 2004). We also show synthetic line profiles for different stellar abundances computed with the local thermodynamic equilibrium (LTE) code MOOG (Sneden 1973), adopting the atomic line data from the Vienna Atomic Line Database (VALD; Piskunov 1995) and using a grid of LTE model atmospheres (Kurucz 1993).

In order to perform the chemical analysis of the secondary star we used a technique which combines a grid of synthetic spectra and a $\chi2$-minimization procedure that includes Monte-Carlo simulations (González Hernández et al. 2004, 2005). First, we inspected the observed spectrum in order to select the most suitable features for a chemical abundance determination. We identified nine spectral features containing in total 30 lines of Fe I and 8 lines of Ca I with excitation potentials between 1 eV and 5 eV. The oscillator strengths of the relevant spectral lines were checked via spectral synthesis against the solar atlas (Kurucz et al. 1984). We then generated a grid of about one million synthetic spectra of each of these features, varying as free parameters the star effective temperature (T_{eff}), surface gravity ($\log g$), and metallicity ([Fe/H]), together with the veiling from the accretion disk which was assumed to be a linear function of wavelength, and thus described by two additional parameters. Iron abundances were varied in the range $-1.5 <$ [Fe/H] < 1 whereas the Ca abundance was fixed, for each given iron abundance, according to the Galactic trend of Ca (Bensby et al. 2005) for [Fe/H] < 0, and fixed to [Ca/Fe] $= 0$ in the range $0 <$ [Fe/H] < 1. A rotational broadening of 100 $\mathrm{km\,s^{-1}}$ and a limb darkening $\epsilon = 0.8$ were adopted. The microturbulence (ξ) was computed using an experimental expression as a function of effective temperature and surface gravity (Allende Prieto et al. 2004).

We compared, using a $\chi2$-minimization procedure, this grid with 1000 realizations of the observed spectrum. Using a bootstrap Monte-Carlo method, we found the most likely values $T_{\mathrm{eff}} = 4700 \pm 100$ K, $\log(g/\mathrm{cm\ s^2}) = 4.6 \pm 0.3$, [Fe/H] $= 0.2 \pm 0.2$, and a disk veiling (defined as $F_{\mathrm{disk}}/F_{\mathrm{total}}$) of less than 40% at 5000 Å and decreasing toward longer wavelengths. The (1σ) uncertainty in the iron-abundance determination takes into account the uncertainties in the stellar and veiling parameters. The effective temperature and surface gravity are consistent with previous spectral classifications and similarly the reported veiling values (Torres et al. 2004). Using the derived stellar and veiling parameters, we analyzed several spectral regions where we had identified various lines of Fe, Ca, Al, Mg and Ni. Abundances of all the elements are listed in Table 1. The 1σ uncertainty in the abundance determination takes into account uncertainties in the stellar and veiling parameters.

Remarkably, we find a metallicity higher than solar, which is extremely atypical of halo stars (Allende Prieto et al. 2006). In Figure 1 we show the best-fit synthetic spectrum to various features in two different spectral regions, and for comparison, a model with twenty-five times lower metal content. Notice the inadequacy of low-metallicity models to reproduce the observed features, even in the extreme case that no veiling is considered (adding veiling would make the discrepancy much worse). An iron abundance of [Fe/H] $= -1.2$ is more than 6σ away from the best-fit solution ([Fe/H] $= 0.18$), and hence very unlikely. We have also found that abundances of Al, Ca, Mg, and Ni are higher than solar (see Table 1). In Figure 2, we show that the abundance ratios of these elements with respect to iron are consistent with those of stars in the solar neighborhood from Gilli et al. (2006). We have also determined an upper limit to the Li abundance $\log \epsilon(\mathrm{Li})_{\mathrm{LTE}} = \log[N(\mathrm{Li})/N(\mathrm{H})]_{\mathrm{LTE}} + 12 \leq 1.61 \pm 0.25$ using the Li 6708 Å line. This value seems to be lower that typical high Li abundances measured in other late-type secondary stars in soft X-ray transients whose origin is still an open question (Martín et al. 1994).

4. Discussion and Conclusions

If we include the metallicity distribution of halo and thick-disk stars (Allende Prieto et al. 2006) and thin-disk stars (Allende Prieto et al. 2004) in the equations based on kinematics for establishing the relative likehoods of belonging to the halo, thick disk, or thin disk (Bensby et al. 2003), the probability that a star with the Galactic space velocity components of this system (Mirabel et al. 2001; $U = -105 \pm 16$ km s^{-1}, $V = -98 \pm 16$ km s^{-1}, $W = -21 \pm 10$ km s^{-1}) and metallicity [Fe/H] $= 0.18$ belongs to the Galactic halo is less than 0.1%. Moreover, the kinematics alone suggest thick-disk rather than halo membership, although the high metallicity of the secondary star favors thin-disk membership. If, however, the progenitor was a massive star in the halo or thick disk, the high metallicity of the secondary rules out the hypothesis that the black hole was formed by direct collapse of the massive star; instead, a supernova explosion origin is strongly suggested.

Given its present orbital distance from the black hole ($a_{\mathrm{c}} \approx 3$ R$_{\odot}$, Wagner et al. 2001), it is plausible that the secondary star captured a significant fraction of the matter ejected in a supernova explosion. The chemical composition of the secondary may provide crucial information on nucleosynthesis in the progenitor and the formation mechanism of the black hole. We consider two possible scenarios for the origin of the compact object: either it formed in the Galactic halo or thick disk as a result of the explosion of a metal-poor massive progenitor which enriched the secondary star from the typical abundances of halo/thick-disk stars up to the observed supersolar values, or alternatively, it formed in the Galactic thin disk with a natal kick imparted during the supernova explosion which propelled the binary into its current orbit.

In the first case, the similarity with the kinematics of halo and thick-disk stars makes unnecessary a significant kick during the black hole formation process. However, since the typical metallicities of halo stars and thick-disk stars are significantly lower than solar, it is required that the secondary captured enough matter from the ejecta to reach the current abundances. A metal-poor $\sim$1 M$_{\odot}$ secondary star, initially placed at an orbital distance of $\sim$6 R$_{\odot}$ (after tidal circularization of the orbit), would need to capture roughly 5–10% of the matter ejected in a spherically symmetric core-collapse supernova explosion of a 16 M$_{\odot}$ helium core to achieve the observed iron abundance. We have considered supernova and hypernova models of metal-poor progenitors with different masses, metallicities, mass cuts (i.e., the mass above which the matter is expelled at the time of the supernova explosion), fallback (i.e., amount of mass which is eventually accreted by the compact core), and mixing (Umeda & Nomoto, 2002, 2005; Tominaga, Umeda & Nomoto 2006, in preparation), and assumed that all the fallback material is well mixed with the ejecta. We find that a sufficiently large Fe enrichment is possible for mass cuts in the range 2–4 M$_{\odot}$ [and explosion energies $(1 - 30) \times 10^{51}$ ergs]. The abundance ratios of the other elements are only marginally reproduced by these models. An origin of XTE J1118+480 in the Galactic halo or in the Galactic thick disk cannot be discarded by the present observations, nor can it be confirmed. Further higher-quality observations and extensive model calculations are required to fully explore this possibility. Further details of analysis will put together in Gonález Hernández et al. (2006, in preparation).

In the second scenario, the system had to acquire a peculiar space velocity of $\sim 180\ \mathrm{km\,s^{-1}}$, to change from a Galactic thin disk orbit to the currently observed orbit (Gualandris et al. 2005), requiring an asymmetric kick. Such kicks imparted during the birth of nascent neutron stars, due to asymmetric mass ejection and/or an asymmetry in the neutrino emission (Lai et al. 2001), have been proposed to explain the large transverse motions of neutron stars in the plane of the sky (Lyne & Lorimer 1994). The black hole could have formed in a two-stage process where the initial collapse led to the formation of a neutron star accompanied by a substantial kick and the final mass of the compact remnant was achieved by matter that fell back after the initial collapse as proposed to explain the origin of the black hole in Nova Sco 1994 (Podsiadloski et al. 2002; Brandt et al. 1995).

Spherically symmetric explosion models are able to explain the observed metal enrichment. A modest amount of ejecta (~ 0.02) $\mathrm{M_\odot}$ captured by a secondary with initial solar abundance is sufficient if vigorous mixing (Kifonidis et al. 2000) between the fallback matter (which is necessarily large given the mass of the black hole) and the ejecta took place. In this scenario the black hole would be formed in a mild explosion with fallback as in collapsar models (MacFadyen et al. 2001) associated with rapidly rotating massive stars. However, in the pure spherical supernova explosion scenario for XTE J1118+480, the maximum allowed ejected mass to keep the secondary star gravitationally bound is $\Delta M \approx 8\ \mathrm{M_\odot}$. This leads to a system velocity of $\sim 60\ \mathrm{km\,s^{-1}}$ (there could be extreme cases with system velocities as high as $\sim 100\ \mathrm{km\,s^{-1}}$ requiring very *special* model parameters such as higher secondary and black hole masses just after the explosion; see further details in Sec. 3.2 of Gualandris et al. 2005), much lower than the observed value, and a neutrino-induced kick is required if we are to explain the kinematics of the system.

The chemical composition of the ejecta in a non-spherically symmetric supernova explosion is strongly dependent on direction. In particular, if we assume that the jet is collimated perpendicular to the orbital plane of the binary, where the secondary star is located, elements such as Ti, Ni, and Fe are mainly ejected in the jet direction, while Al, O, Si, S, and Mg are preferentially ejected near the equatorial plane of the helium star (Maeda et al. 2002). Using predictions for an aspherical explosion model of a 16 $\mathrm{M_\odot}$ He core metal-rich progenitor, we can explain the observed abundances in the secondary. Complete lateral mixing (Podsiadlowski et al. 2002) is required to account for the similar enhancement of Mg and Ni and the observed abundances can be reproduced for all mass cuts in the range 2–8 $\mathrm{M_\odot}$.

It is therefore plausible that the black hole in XTE J1118+480 formed in the Galactic thin disk from a massive metal-rich progenitor and was launched into its current orbit either by mass ejection in an asymmetric supernova/hypernova explosion or by a neutrino-induced kick. In addition, ultraviolet observations of the accretion disk in this system suggest that the material accreted onto the compact object is substantially CNO processed (Haswell et al. 2002), indicating that the zero-age mass of the secondary star could have been $\sim 1.5\ \mathrm{M_\odot}$. By means of binary evolution calculations this may constrain the age of the system in the range 2–5.5 Gyr (Gualandris et al. 2005). Future chemical studies of the secondary star during periods of quiescence may provide accurate abundances of elements (e.g., C, Ti, Si) whose lines either are not available in the observed spectrum or are present in spectral regions where the signal-to-noise ratio is too low for an accurate chemical analysis. These may reveal further details of the formation mechanism of the black hole in this system.

We are grateful to Hideyuki Umeda, Ken'ichi Nomoto, and Nozomu Tominaga for sending us their explosion models for metal-poor and metal-rich progenitors and several programs for our model computations. We also thank Keiichi Maeda for providing us with his aspherical explosion models, and for helpful discussions. We are grateful to Tom Marsh for the use of the MOLLY analysis package, to Jorge Casares for his helpful comments on different aspects of this work, and to Ryan J. Foley for assistance with the observations. We also thank the referee for helpful comments. The W. M. Keck Observatory is operated as a scientific partnership among the California Institute of Technology, the University of California, and

NASA; it was made possible by the financial support of the W. M. Keck Foundation. This work has made use of the VALD database and IRAF facilities. It was funded in part by Spanish Ministry project AYA2005-05149 and by US National Science Foundation grant AST-0307894. We dedicate this paper to the memory of our dear friend and collaborator E. T. Harlaftis, whose life was tragically cut short by a snow avalanche on 13 February 2005.

REFERENCES

Allende Prieto, C., Barklem, P. S., Lambert, D. L., & Cunha, K. 2004, A&A, 420, 183

Allende Prieto, et al. 2006, ApJ, 636, 804

Bensby, T., Feltzing, S., Lundström, I., & Ilyin, I. 2005, A&A, 433, 185

Brandt, W. N., Podsiadlowski, Ph., & Sigurdsson, S. 1995, MNRAS, 277, L35

Gilli, G., Israelian, G., Ecuvillon, A., Santos, N. C., & Mayor, M. 2006, A&A, in press

González Hernández, J. I., Rebolo, R., Israelian, G., Casares, J., Maeda, K., Bonifacio, P., & Molaro, P. 2005, ApJ, 630, 495

González Hernández, J. I., Rebolo, R., Israelian, G., Casares, J., Maeder, A., & Meynet, G. 2004, ApJ, 609, 988

Gualandris, A., Colpi, M., Portegies Zwart, S., & Possenti, A. 2005, A&A, 618, 845

Haswell, C. A., Hynes, R. I., King, A. R., & Schenker, K. 2002, ApJ, 332, 928

Israelian, G., Rebolo, R., Basri, G., Casares, J., & Martín, E. L. 1999, Nature, 401, 142

Kifonidis, K., Plewa, T., Janka, H.-Th., & Mller, E. 2000, A&A, 531, L123

Kurucz, R. L. ATLAS9 Stellar Atmospheres Programs and 2 km s^{-1} Grid. (CD-ROM, Smithsonian Astrophysical Observatory, Cambridge, 1993).

Kurucz, R. L., Furenild, I., Brault, J., & Testerman, L. 1984, Solar Flux Atlas from 296 to 1300 nm, NOAO Atlas 1 (Cambridge: Harvard Univ. Press)

Lai, D., Chernoff, D. F., & Cordes, J. M. 2001, ApJ, 549, 1111

Lyne, A. G., & Lorimer, D. R. 1994, Nature, 369, 127L

MacFadyen, A. I., Woosley, S. E., & Heger, A. 2001, ApJ, 550, 410

Maeda, K., Nakamura, T., Nomoto, K., Mazzali, P. A., Patat, F., & Hachisu, I. 2002, ApJ, 565, 405

Martín, E. L., Rebolo, R., Casares, J., & Charles, P. A. 1994, ApJ, 435, 791

McClintock, J. E., et al. 2003, ApJ, 593, 435

Mirabel, I. F., Dawan, V., Mignani, R. P., Rodrigues, I., & Guglielmetti, F. 2001, Nature, 413, 139

Piskunov, N. E., Kupka, F., Ryabchikova, T. A., Weiss, W. W., & Jeffery, C. S. 1995, A&AS, 112, 525

Podsiadlowski, P., Nomoto, K., Maeda, K., Nakamura, T., Mazzali, P., & Schmidt, B. 2002, ApJ, 567, 491

Remillard, R., Morgan, E., Smith, D., & Smith, E. 2002, IAU Circ. No. 7389

Sheinis, A. I., et al. 2002, PASP, 114, 851

Sneden, C. 1973, PhD Dissertation (Univ. of Texas at Austin)

Torres, M. A. P., et al. 2004, ApJ, 612, 1026

Umeda, H., & Nomoto, K. 2002, ApJ, 565, 385

Umeda, H., & Nomoto, K. 2005, ApJ, 619, 427

Wagner, R. M., et al. 2001, ApJ, 556,42

This 2-column preprint was prepared with the AAS LaTeX macros v5.2.

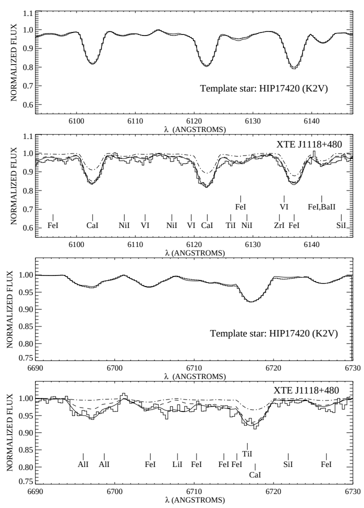

Fig. 1.— Best synthetic spectral fits to the ESI spectrum of the secondary star in the XTE J1118+480 system (second and bottom panels) and the same for a template star (properly broadened) taken from Allende Prieto et al. (2004) shown for comparison (top and third panels). Synthetic spectra are computed for typical abundances for a halo star ([Fe/H] $= -1.2$, dashed-dotted blue line), solar abundances ([Fe/H] $= 0$, dashed green line), and best-fit abundances (solid red line). In addition, note that for solar and best-fit abundances we have applied to the synthetic spectra the corresponding values for the veiling according to the solution found with the fitting procedure. However, for the low-metallicity synthetic spectra, we have not assumed any veiling.

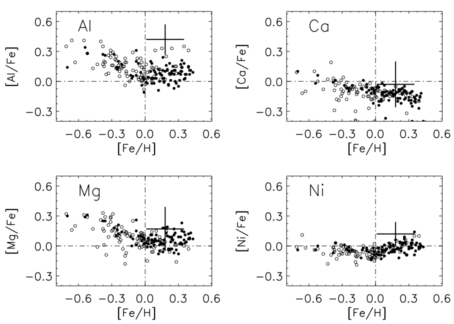

Fig. 2.— Abundance ratios of the secondary star in XTE J1118+480 (blue wide cross) in comparison with the abundances of G and K metal-rich dwarf stars. Galactic trends were taken from Gilli et al. (2006). The size of the cross indicates the uncertainty. Filled and empty circles correspond to abundances for planet host stars and stars without known planet companions, respectively. The dashed-dotted lines indicate solar abundance values.

TABLE 1
ABUNDANCES IN THE SECONDARY STAR

Parameter	Al	Ca	Mg	Fe	Ni
[X/H]	0.60	0.15	0.35	0.18	0.30
Δ[X/H]	0.20	0.23	0.25	0.17	0.21

NOTE.—Element abundances (calculated assuming LTE) are $[X/H] = \log[N(X)/N(H)]_{\rm star} - \log[N(X)/N(H)]_{\rm Sun}$, where $N(X)$ is the number density of atoms. Uncertainties, Δ[X/H], are 1σ and take into account uncertainties in the stellar and veiling parameters.